Optical trapping of dielectric nanoparticles in resonant cavities

Juejun Hu,[1,2,*] Shiyun Lin,[3] Lionel C. Kimerling,[1] and Kenneth Crozier[3]
[1]*Microphotonics Center, Massachusetts Institute of Technology, Cambridge, Massachusetts 02139, USA*
[2]*Department of Materials Science & Engineering, University of Delaware, Newark, Delaware 19716, USA*
[3]*School of Engineering and Applied Science, Harvard University, Cambridge, Massachusetts 02138, USA*
(Received 20 August 2009; published 16 November 2010)

We theoretically investigate the opto-mechanical interactions between a dielectric nanoparticle and the resonantly enhanced optical field inside a high Q, small-mode-volume optical cavity. We develop an analytical method based on open system analysis to account for the resonant perturbation due to particle introduction and predict trapping potential in good agreement with three-dimensional (3D) finite-difference time-domain (FDTD) numerical simulations. Strong size-dependent trapping dynamics distinctly different from free-space optical tweezers arise as a consequence of the finite cavity perturbation. We illustrate single nanoparticle trapping from an ensemble of monodispersed particles based on size-dependent trapping dynamics. We further discover that the failure of the conventional dipole approximation in the case of resonant cavity trapping originates from a new perturbation interaction mechanism between trapped particles and spatially localized photons.

DOI: 10.1103/PhysRevA.82.053819 PACS number(s): 42.50.Wk, 42.60.Da, 87.80.Cc

I. INTRODUCTION

Optical trapping and manipulation of micron-sized objects are becoming increasingly important techniques in biotechnology and micro-fabrication due to their noncontact nature and inherent high precision [1–5]. Stable trapping of nanoparticles (<100 nm), however, still remains a major challenge as high optical power is required using either free space optics or evanescent trapping configurations, a consequence of the rapid decrease of optical force when scaling down the particle size.

Resonant cavity trapping has been theoretically proposed [6–8] and recently experimentally demonstrated [9–12] as a promising solution for nanoparticle manipulation. In a resonant cavity, the optical field is significantly enhanced and thus effectively reduces the power threshold for stable trapping. The resonant cavity enhancement factor scales with Q/V [13], suggesting that high-Q nanocavities with a small-mode volume, such as photonic crystal (PC) cavities, are particularly attractive for optical trapping applications. In addition, the scattering force component becomes negligible compared to the gradient force component in a standing wave PC cavity. Particles can be therefore stably trapped at field extrema, rather than being propelled along the light propagation direction. This facilitates subsequent analysis using sensitive cavity-enhanced spectroscopic techniques such as fluorescence or Raman spectroscopy.

Despite the immense application potential of resonant cavities for optical trapping, quantitative study of the opto-mechanical interactions between trapped dielectric particles and the optical field inside a resonant cavity is scarce to date. Furthermore, we notice that field perturbation due to the introduction of a particle also becomes strongly enhanced in a nanocavity with a large Q/V ratio, given the high field concentration. This important distinction invalidates the conventional dipole approximation formulation [14] in a resonant cavity trapping setting, and an alternative theory is thus highly desirable. In this paper, we apply open system analysis to address the cavity field perturbation and analyze particle trapping behavior.

II. THEORY

In the following analysis, we consider dielectric particle trapping inside a generic standing wave resonant cavity coupled to an excitation field oscillating at a given frequency ω. When coupling to the excitation field is small, the cavity can be treated as a closed system and the photon number or field intensity residing in the cavity is fixed [9,15]. We have proven that this closed system approach applied to particle trapping inside a resonant cavity is mathematically equivalent to the conventional dipole approximation (see Appendix A). However, in the event that the coupling to an external field becomes non-negligible, photon numbers inside the resonant cavity may be altered due to perturbations arising from particle introduction. Therefore, the open system analysis approach, given below, is a more appropriate description of a loaded cavity.

Assuming linear polarizability, the time-averaged polarization energy associated with the presence of a nonmagnetic particle is given by

$$\Phi = -\frac{1}{4V_p}\mathrm{Re}(\alpha)\int_{V_p}|E|^2 dV, \tag{1}$$

where E denotes the electric field complex amplitude of the resonant cavity mode, α is the polarizability of particle, and the integral is carried out over the particle volume V_p. The polarization energy Φ can be expressed in terms of the excitation light power P as

$$\Phi = -\frac{T\mathrm{Re}(\alpha)QP}{4\omega V_p}\int_{V_p}|E_N|^2 dV = -\frac{T\mathrm{Re}(\alpha)QP}{4\omega}|E_N|^2, \tag{2}$$

where Q is the cavity quality factor, ω is the excitation light frequency, and T represents the fractional power coupling coefficient into the resonant cavity. The field E_N is the dimensionless eigenmode of the unperturbed resonant cavity

*hujuejun@udel.edu

normalized so that $\int_{\text{cavity}} |E_N|^2 dV = 1$, and is a function of spatial coordinates. The second equality holds when the particle is sufficiently small to be treated as a dipole *in free space*. Note that this qualification does not necessarily imply that the conventional dipole approximation can be applied to solve optical force exerted on the particle when it is placed *in a resonant cavity*, as the resonant cavity perturbation effect detailed below can invalidate the conventional dipole approximation. Unlike closed system analysis, the coupling coefficient T is explicitly incorporated in Eq. (2). Two terms with the dimension of force arise by taking the spatial derivative of Φ:

$$-\vec{\nabla}\Phi = \frac{\text{Re}(\alpha)P}{4\omega}[QT \cdot \vec{\nabla}|E_N|^2 + |E_N|^2 \cdot \vec{\nabla}(QT)]. \quad (3)$$

The first term in the parenthesis is analogous to the gradient force term in the dipole approximation, modulated by the coupling coefficient to account for the resonant field perturbation. Position-dependent polarization energy change due to the second term in the parenthesis, however, is simply the manifestation of equilibrium photon number variation inside the cavity due to particle position change. The associated polarization energy variation is compensated by the transient change of the coupling coefficient T as is dictated by cavity dynamics, and is purely of electromagnetic nature. As a consequence, the second term does not contribute to optical force. We shall also note that the additional cavity coupling term T in the formulation is a consequence of particle-induced photon number modulation in the cavity, and is fundamentally different from excitation of high-order multipole terms (see the discussion section and Fig. 5 in Appendix B).

Since the resonance line shape can be well approximated by a Lorentzian function, the incident-wavelength-dependent coupling coefficient T is determined by the relative detuning of excitation wavelength λ from the resonant wavelength λ_r of the cavity in the presence of particle:

$$T(\lambda) = \frac{\lambda_r^2}{\lambda_r^2 + 4Q^2(\lambda - \lambda_r)^2}, \quad (4)$$

where the particle-induced shift of λ_r with respect to the "empty-cavity" resonant wavelength λ_{r0} may be calculated via cavity perturbation theory. Notably when the index contrast between the particle and the medium is high, that is, in case $(\varepsilon - \varepsilon_m)$ is comparable to ε_m (ε_m denotes the dielectric constant of surrounding medium), the conventional cavity perturbation theory becomes invalid. Based on the Hellmann-Feynman theorem [16], we derive an alternative formalism (see Appendix C):

$$\lambda_r = \lambda_{r0} + \frac{\lambda_{r0}|E_N|^2}{2\int_{\text{cavity}} \varepsilon_c |E_N|^2 dV}\text{Re}(\alpha). \quad (5)$$

Here ε_c denotes the dielectric constant distribution of the resonant cavity. Furthermore, when the particle is optically absorbing, the cavity Q factor becomes a function of particle position in the cavity, which leads to [17]

$$\frac{1}{Q} = \frac{1}{Q_0} + \frac{\int_{\text{cavity}} \varepsilon_c |E_N|^2 dV}{\varepsilon'' V_p |E_N|^2}. \quad (6)$$

Here Q_0 represents the unperturbed cavity Q factor, and ε'' is the imaginary part of the complex dielectric constant of particle. For nanoparticles with radius <100 nm, cavity Q-factor deterioration due to scattering is usually much smaller compared to the optical absorption effect and therefore can be neglected.

Combining Eqs. (3) and (4) yields the optical gradient force F as a function of incident light power and wavelength:

$$F(P,\lambda) = \frac{\text{Re}(\alpha)QP}{4\omega}\frac{\lambda_r^2}{\lambda_r^2 + 4Q^2(\lambda - \lambda_r)^2} \cdot \vec{\nabla}|E_N|^2. \quad (7)$$

The spatial dependence of optical force is implicitly contained in the field spatial derivative term and in the cavity Q factor when the particle is optically absorbing [see Eq. (6)].

The mathematical formulation of α at nonzero frequencies, however, is not trivial. A rigorous treatment invokes multipole effects [18]. In the electric dipolar limit, the effective polarizability of a spherical particle can be calculated from the Mie theory and is given by

$$\alpha(k,r) = i\varepsilon_m \frac{6\pi}{k^3} \frac{\sqrt{\varepsilon}\Psi_1(\sqrt{\varepsilon/\varepsilon_m}kr)\Psi_1'(kr) - \sqrt{\varepsilon_m}\Psi_1'(\sqrt{\varepsilon/\varepsilon_m}kr)\Psi_1(kr)}{\sqrt{\varepsilon}\Psi_1(\sqrt{\varepsilon/\varepsilon_m}kr)\xi_1'(kr) - \sqrt{\varepsilon_m}\Psi_1'(\sqrt{\varepsilon/\varepsilon_m}kr)\xi_1(kr)}, \quad (8)$$

where k is the wave vector of the excitation light, r is the sphere radius, Ψ_1 and ξ_1 are Ricatti-Bessel functions, and ε is the complex dielectric constant of particle. For nonspherical particles, Draine's formulation of polarizability including a radiation damping term [19] provides a good approximation.

By comparison we can see that when the coupling coefficient T approaches unity, that is, when the following condition is satisfied,

$$\text{Re}(\alpha)Q\frac{|E_N|^2}{2\int_{\text{cavity}} \varepsilon_c |E_N|^2 dV} \approx \frac{\text{Re}(\alpha)Q}{\varepsilon_c V_c} \ll 1, \quad (9)$$

where V_c gives the cavity mode volume, and the open cavity analysis Eq. (7) converges with the conventional dipole approximation. Starting from Eq. (7), we define the condition $\text{Re}(\alpha)Q/\varepsilon_c V_c < 0.1$ as a semiempirical criterion for the validity of the conventional dipole approximation. Notably, unlike the conventional applicability condition of dipole approximation $r \ll \lambda$, Eq. (9) does not explicitly incorporate wavelength dependence. Therefore, large deviation from the dipole approximation may arise in a high-Q nanocavity with a small-mode volume, even for particles much smaller than the wavelength. For instance, in a water-filled PC cavity with a moderate $Q = 10\,000$ and a mode volume $V_c = 1\ \mu\text{m}^3$ operating at 1550-nm telecommunication wavelength, a spherical dielectric particle with a refractive index of 1.5 needs to have a radius r of 35 nm ($\lambda/r \sim 44$) or smaller to

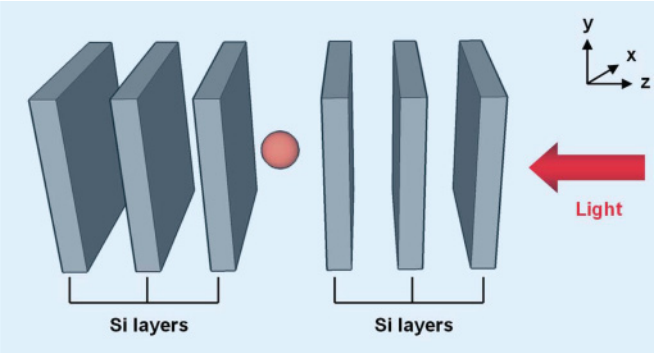

FIG. 1. (Color online) Schematic illustration of a 1D Bragg cavity used to demonstrate the resonant cavity trapping principles. For the specific example in this figure, each Bragg mirror consists of three high-index silicon layers and the whole device is immersed in water.

meet the condition $\mathrm{Re}(\alpha)Q/\varepsilon_c V_c < 0.1$. By comparison, it has been found that dipole approximation holds up to $\lambda/r \sim 10$ with high accuracy in an evanescent trapping configuration [20].

III. PARTICLE TRAPPING DYNAMICS IN A 1D CAVITY

Here we use a one-dimensional (1D) photonic crystal cavity (Bragg cavity stack) as a vehicle to illustrate the fundamental properties of resonant cavity particle trapping, although the trapping dynamics derived from this 1D example are equally applicable to cavities with two-dimensional (2D) or 3D optical confinement. The cavity under consideration consists of a half-wavelength water-filled ($n_{\mathrm{water}} = 1.33$) defect layer sandwiched between two quarter-wavelength stack Bragg mirrors (Fig. 1). We choose silicon ($n_{\mathrm{Si}} = 3.46$) as the high index medium in the Bragg mirrors. The cavity is designed to exhibit a Fabry-Perot optical resonance at a vacuum wavelength of 1 μm. The cavity Q factor is varied by adjusting the number of layers in the mirror stack. For convenience, optical absorption in the layers is neglected without losing generality. We assume plane waves within the unperturbed cavity, whose cross section is taken as 600 $\times$ 600 nm. The excitation power launched into the cavity is fixed at 5 mW throughout this paper.

We performed 3D FDTD simulations with electric or magnetic wall boundary conditions to determine the field profile of the resonant mode when a spherical silicon nanoparticle is placed at different locations along the z axis inside the cavity. The position of the particle in the x-y plane is unimportant given the symmetry of the cavity and plane wave excitation. The Maxwell stress tensor is then employed to derive the optical force based on the (FDTD-simulated) perturbed field pattern. In parallel, the transfer matrix method is applied to calculate the unperturbed optical field inside the cavity, which serves as the input to both the dipole approximation and the open cavity analysis. Results obtained by the three techniques are directly compared.

To facilitate the comparison, we examine the spherical particle case. In our first example, we compare the optical force exerted on a silicon particle ($\varepsilon = 12$) offset by 90 nm from the center of the cavity along the z axis. The cavity is illuminated by a plane wave with a vacuum wavelength of 1 μm. Figure 2(a) shows the optical force and trapping potential calculated using the open cavity analysis, 3D FDTD simulations, and the conventional dipole approximation. The maximum relative deviation between the open cavity analysis and FDTD simulations is within 10%, and is mainly due to (1) the finite size of the mesh used in the FDTD calculations, which accounts for ~5% error according to a numerical convergence study we performed; and (2) neglecting multipole polarization effects, which would be most pronounced for

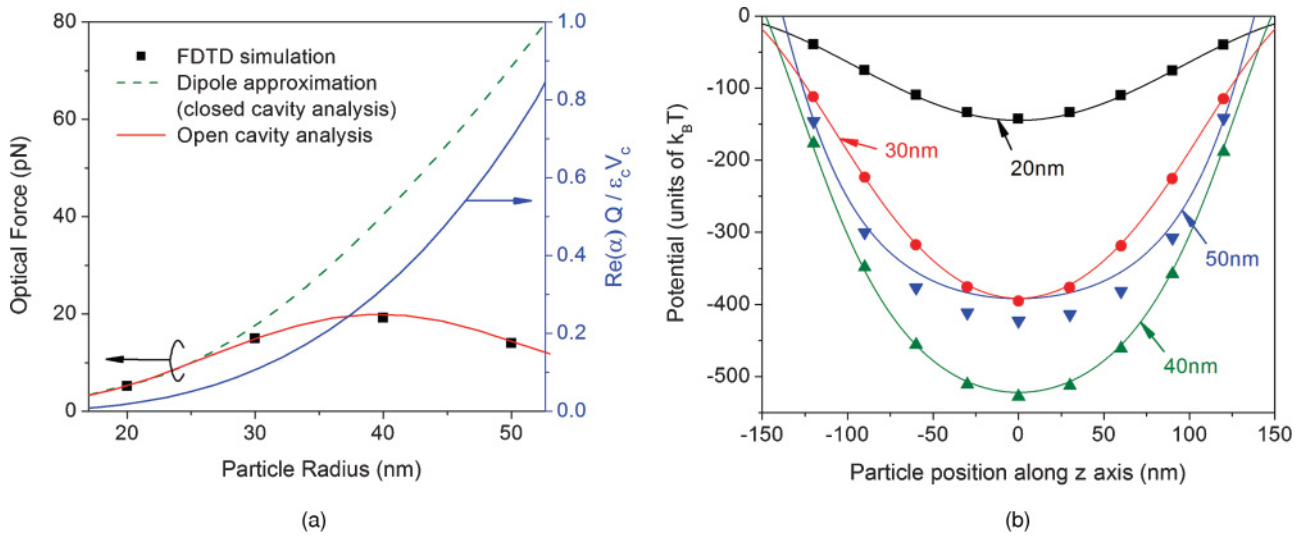

FIG. 2. (Color online) (a) Optical force exerted on a spherical particle located in the cavity illustrated in Fig. 1. Particle is offset by 90 nm from the center of the cavity along the z axis. Right-side axis gives the dimensionless parameter $\mathrm{Re}(\alpha)Q/\varepsilon_c V_c$: the deviation between dipole approximation and the open cavity analysis Eq. (7) scales with its magnitude. (b) Optical trapping potential profile experienced by particles of different radii, given in $k_B T \sim 0.026$ eV; the solid lines correspond to the open cavity analysis, and the solid symbols are FDTD simulation results, calculated by integrating the optical force along the z axis.

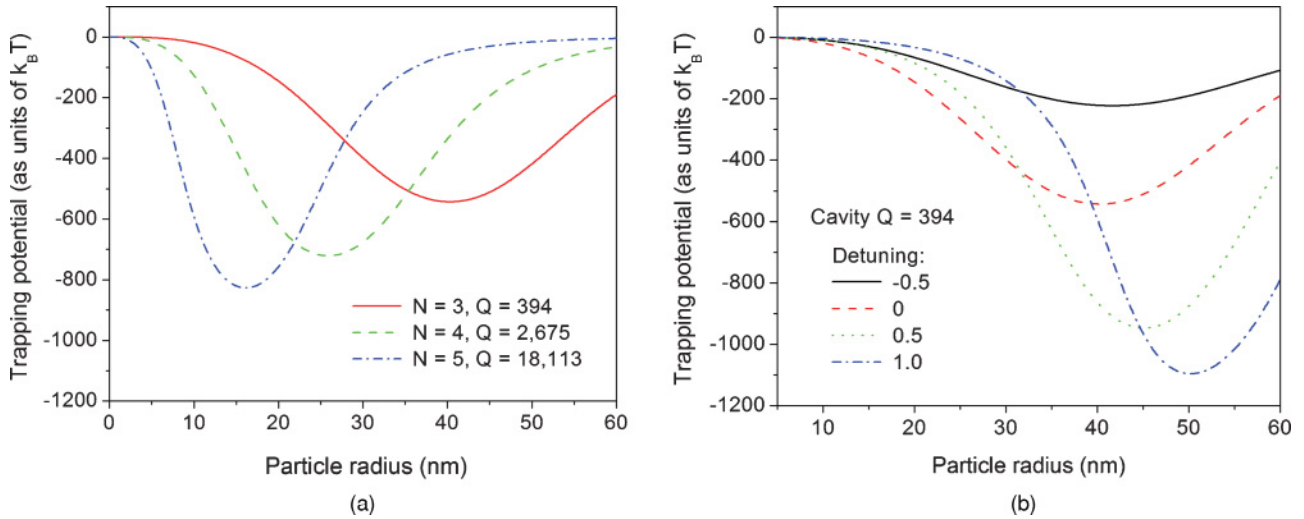

FIG. 3. (Color online) (a) Single-particle trapping potential in 1D cavities with different numbers of Bragg mirror pairs N and hence different Q factors. (b) Trapping potential in a cavity shown in Fig. 1 ($N = 3$) as a function of particle radius; the detuning is given as the relative shift between the cavity resonant wavelength and the excitation wavelength, and is expressed as the fraction of resonant peak full width at half maximum (FWHM).

large particles [18]. Consistent with the condition specified in Eq. (9), the dipole approximation agrees with the open cavity analysis only when the dimensionless parameter $\mathrm{Re}(\alpha)Q/\varepsilon_c V_c$ is much smaller than unity. When the parameter becomes comparable to 1, introduction of the particle into the cavity leads to non-negligible resonance detuning. Consequently, the photon number and the optical field amplitude inside the cavity decrease, a back-action phenomenon not captured in the closed cavity approach. According to Eq. (5), such cavity perturbation is most pronounced when the particle position overlaps with the field maxima. Therefore, the underestimation of the optical force by the conventional dipole approximation, compared to the open cavity approach, is most significant when the particle is close to the center of cavity. Overall, the net effect results in a single-particle trapping potential with a "flattened" bottom shape, as is shown in Fig. 2(b). In addition, the enhanced cavity perturbation as particle size increases ultimately overtakes the polarizability increase, leading to a peak value of optical force magnitude and trapping potential as a function of particle radius. This size-selective phenomenon clearly distinguishes resonant cavity trapping from conventional optical tweezers using free-space or evanescent wave geometry, which preferentially trap large particles. This characteristic constitutes the basis of a wide array of intriguing applications that we will discuss in Sec. IV.

Since resonance perturbation affects the opto-mechanical interactions, it is expected that the trapping potential will critically depend on cavity Q factor as well as wavelength detuning of the excitation light source from the resonant wavelength. Such functional dependencies are plotted in Figs. 3(a) and 3(b), for different cavity Q factors and wavelength detuning values. Clearly, optical resonant cavities can be engineered to capture nanoparticles of different sizes in a selective manner by exploiting this size-dependent trapping potential depth. Further, Fig. 3(b) suggests that similar size selectivity may also be achieved in the *same* cavity structure by adjusting the excitation wavelength. This feature, referred to as "self-induced trapping" [7], provides increased operation flexibility for resonant cavity opto-mechanical devices.

Here we further illustrate the capture of a *single* nanoparticle in a resonant cavity via optical force, in addition to the potential applications discussed earlier of resonant cavity trapping for particle sorting and size-selective manipulation. As shown in Fig. 4, the optical trapping force exerted on a nanoparticle entering a resonant cavity is significantly reduced if there is already one identical particle stably trapped inside the cavity. This is phenomenologically analogous to single electron device operation where the introduction of one electron decreases the occupancy probability of a second electron. This unique characteristic of resonant cavity trapping could enable a novel route toward single-particle trapping within the active volume of an optical cavity, from an ensemble of monodispersed nanoparticles. For instance, such single-particle trapping can be realized by applying a Stokes drag force on the particles (e.g., by adjusting liquid flow velocity through the cavity) to remove the other particle that is much less tightly trapped. It is worth noting that the opto-mechanical interactions involving two particles in a cavity cannot be described by a scalar potential, as the optical force acting on one of the particles becomes nonconservative when the other particle is also in motion. The ability to position a single nanoparticle inside a resonant cavity as is shown here is technically important for a wide spectrum of applications that involve photon-matter interactions. Examples include single dot cavity quantum electrodynamics [21], low-threshold single quantum dot lasers [22], and single molecule analysis using cavity-enhanced spectroscopic techniques [23].

IV. DISCUSSION

The mechanism underlying the failure of the dipolar approximation in the case of resonant cavity trapping warrants

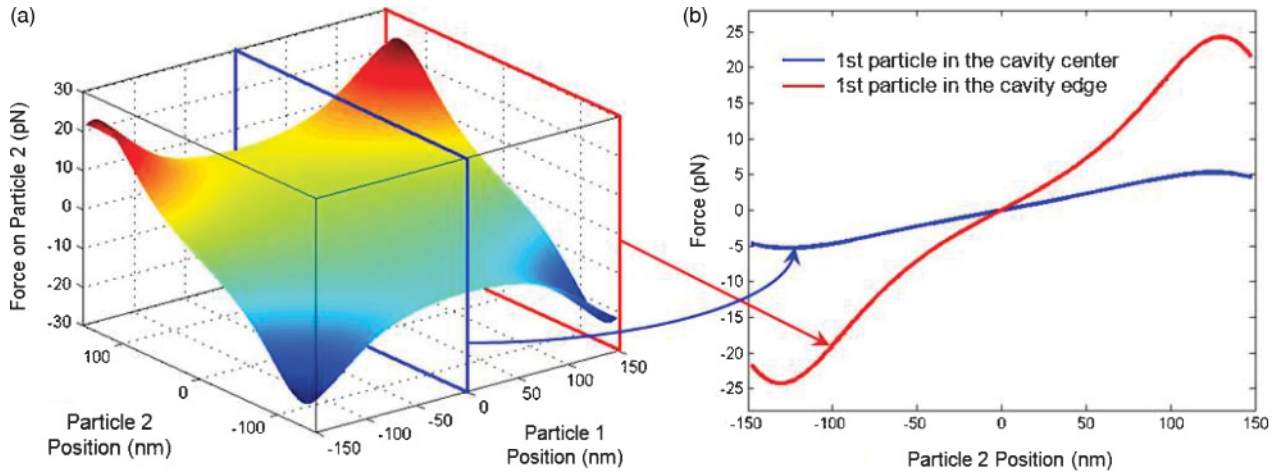

FIG. 4. (Color online) (a) Optical force exerted on a 40-nm-radius particle located in a cavity structure shown in Fig. 1 when another identical particle is also present in the resonant cavity, plotted as a function of the two particles' positions along the z axis. (b) Two cross sections of the plot (a), showing the optical force applied on the second particle when the first particle is in the cavity center and in the cavity edge, respectively.

further inspection. We would like to point out that this failure is not due to higher-order multipole effects. This statement suggests that incorporation of higher-order expansion terms of the optical field and particle polarization, a commonly used technique for refining the accuracy of dipole approximation in force calculations [24], cannot eliminate the discrepancy between the dipole approximation and the Maxwell stress tensor method (see Appendix B). This fact can also be illustrated in the 1D trapping example, where the optical force becomes a function of cavity mode volume. Therefore particles placed in two 1D cavities with different cross-sectional areas but otherwise identical experience different magnitudes of optical force, a result completely unexpected by the aforementioned higher-order multipole expansion approach given the identical longitudinal field profile in the two cavities.

We show that such a discrepancy stems from the 3D spatial localization of photons in a resonant cavity, a characteristic that fundamentally delineates resonant cavity trapping from conventional trapping schemes such as free-space or evanescent configurations. When photons are confined in a finite volume, two new physical parameters become relevant: optical mode volume and confined photon number. From a quantum mechanical perspective, the former concept describes the localized nature of the photon quantum state, and the latter concept gives the occupancy number of the quantum state under investigation. When a particle is introduced into the system, two perturbation effects result: modification of the quantum state and hence the polarization energy change of a single photon $\hbar d\omega$, as well as the photon occupancy number change dN. The latter mechanism is responsible for the failure of dipole approximation in the case of cavity trapping, while multipole expansion only improves the calculation accuracy of the term $\hbar d\omega$. It is worth pointing out that the occupancy number variation dN is generally inversely proportional to the optical mode volume, a conclusion drawn from general perturbation theory. In the absence of photon localization, the term dN vanishes as the mode volume approaches infinity. Therefore multipole expansion generally proves adequate for free-space or waveguide optical manipulation but is insufficient for cavity trapping.

V. SUMMARY

In summary, we derive a general theoretical framework based on open cavity analysis to analytically solve for the optical forces applied to nanoparticles in a resonant cavity setting, where the conventional dipole approximation is invalidated by cavity perturbation. We show that the opto-mechanical interactions in optical cavities exhibit strong size-selective behavior distinct from free-space and evanescent trapping, a unique feature that enables single nanoparticle trapping within the active volume of an optical cavity. Such a unique phenomenon potentially enables simultaneous trapping and analysis of a single biological molecule; it also opens up new fabrication routes toward novel single quantum dot devices.

ACKNOWLEDGMENTS

The authors thank Dr. Xiaochen Sun for providing the transfer matrix simulation code and helpful discussions.

APPENDIX A

Consider a particle placed in a single-mode closed cavity system excited by a monochromatic electromagnetic wave with an angular frequency ω. The single-mode closed cavity condition stipulates that coupling between the resonant mode under investigation and other modes (both guided and radiative modes) is negligible.

The electric field E and the induced dipole moment P of the particle are generally complex numbers with a time dependence represented by an $\exp(i\omega t)$ factor. Assuming linear polarizability, they are connected by the complex polarizability

α at the frequency ω:

$$\vec{P} = \vec{P_0}e^{i\omega t} = \alpha \vec{E} = \alpha \vec{E_0}e^{i\omega t}, \tag{A1}$$

where the overarrow emphasizes the vectorial nature of both the electric field and the induced dipole moment. Generally, E_0 is a function of the spatial coordinates and thus P_0 is also a function of particle position. The time-average differential polarization energy change is

$$\begin{aligned} dW_p &= -\frac{\omega}{2\pi}\int_0^{2\pi/\omega} dt \mathrm{Re}(\vec{E})\mathrm{Re}(d\vec{P}) \\ &= -\frac{1}{4}\mathrm{Re}(\alpha) d|\vec{E_0}|^2. \end{aligned} \tag{A2}$$

The last equality holds since only the electric field amplitude changes along the integration path we consider (electric field amplitude increases from 0 to E_0). The time-averaged polarization energy of the particle is thus given by

$$W_p = \int_0^{E_0} dW_p = -\frac{1}{4}\mathrm{Re}(\alpha)|\vec{E_0}|^2. \tag{A3}$$

Taking the spatial derivative of the particle polarization energy yields the gradient optical force exerted on the particle,

$$\vec{F} = -\vec{\nabla}W_p = \tfrac{1}{4}\mathrm{Re}(\alpha)\cdot\vec{\nabla}|\vec{E_0}|^2, \tag{A4}$$

which leads to the dipole approximation formulation.

Now let's switch to the closed cavity analysis approach, where the total optical energy residing in the cavity is represented by the sum of photon energy:

$$W = N\hbar\omega, \tag{A5}$$

where N is the number of photons residing in this mode and $\hbar$ is the Planck constant. When the resonant cavity is perturbed due to introduction of the particle, the energy change is given by

$$\Delta W = -N\hbar\Delta\omega, \tag{A6}$$

where $\Delta\omega$ is the resonant frequency shift due to introduction of the particle. Further, we notice that energy change can be expressed as the polarization energy associated with the particle. The classical and quantum mechanical pictures should converge, and therefore,

$$\Delta W = W_p, \text{ i.e., } -N\hbar\Delta\omega = \tfrac{1}{4}\mathrm{Re}(\alpha)|\vec{E_0}|^2. \tag{A7}$$

Equation (A7) links the force formulation derived from closed cavity analysis and the dipole approximation:

$$\vec{F} = -N\hbar\vec{\nabla}\omega = \tfrac{1}{4}\mathrm{Re}(\alpha)\cdot\vec{\nabla}|\vec{E_0}|^2. \tag{A8}$$

Therefore, the closed cavity analysis is equivalent to the dipole approximation in a resonant cavity trapping setting.

The resonant frequency shift $\Delta\omega$ can be solved from Eq. (A7), which gives

$$\Delta\omega = -\frac{\omega\mathrm{Re}(\alpha)|\vec{E_0}|^2}{4N\hbar\omega} = -\frac{\omega|\vec{E_0}|^2}{4W}\mathrm{Re}(\alpha). \tag{A9}$$

APPENDIX B

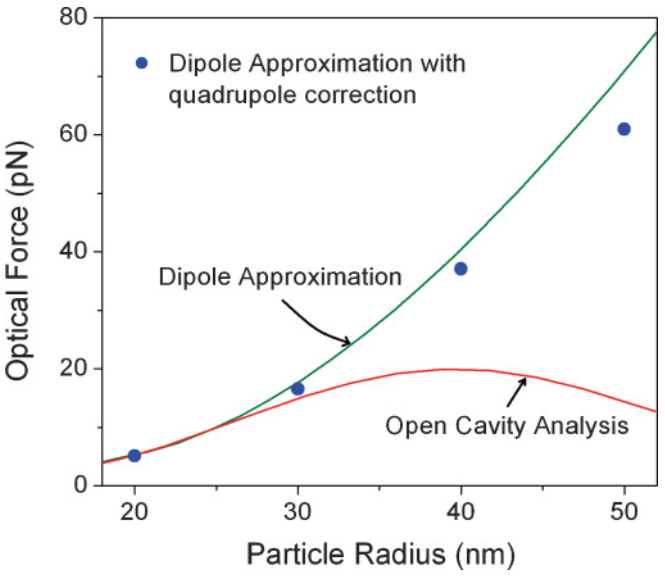

FIG. 5. (Color online) Optical force exerted on a spherical particle located in the cavity illustrated in Fig. 1. Particle is offset by 90 nm from the center of the cavity along the z axis. Thesolid circles give the force results calculated by dipole approximation along with the application of a quadrupole approximation [21]. We see that the discrepancy between the dipole approximation and the Maxwell stress tensor method is not eliminated by the introduction of a quadrupole term, which suggests that the cavity perturbation effect we discuss in this manuscript is fundamentally different from excitation of multipoles.

APPENDIX C

In this section, we aim to derive the resonant frequency shift $\Delta\omega$ caused by introduction of a spherical Rayleigh particle into the cavity. By stipulating the Rayleigh limit, we assume that the particle is spherical, and its radius is much smaller compared to wavelength. The starting point is the Hellmann-Feynman theorem:

$$\frac{d\omega}{d\beta} = -\frac{\omega\int_{V_c}\vec{E_0}^*\left(\frac{d\varepsilon_c}{d\beta}\right)\vec{E_0}dV}{2\int_{V_c}\varepsilon_c|\vec{E_0}|^2dV}, \tag{C1}$$

where ε_c denotes the dielectric constant distribution of the resonant cavity, and β denotes a continuous parameter pertaining to the cavity that is modified due to the perturbation. Here we make the specific choice of β equaling the real part of the particle polarizability:

$$\beta = \mathrm{Re}(\alpha). \tag{C2}$$

Consider a particle with a fixed size, and imagine a process where the dielectric constant of the particle gradually increases from ε_m (dielectric constant of the medium filling the cavity) to ε (the actual dielectric constant of particle); in the same process, the polarizability of the particle also gradually increases from 0 to α (supposedly the actual polarizability of the particle). In this process, $\frac{d\varepsilon_c}{d\beta}$ or $\frac{d\varepsilon_c}{d\mathrm{Re}(\alpha)}$ is a fixed constant inside the particle volume and zero elsewhere. Therefore,

if we assume that the particle is small so the local field inhomogeneity near the particle is negligible (the Rayleigh limit), Eq. (C1) becomes

$$\frac{d\omega}{d\mathrm{Re}(\alpha)} = -\frac{\omega V_p}{2\int_{V_c}\varepsilon_c|\vec{E_0}|^2dV}|\overrightarrow{E_{0,p}}|^2\frac{d\varepsilon_p}{d\mathrm{Re}(\alpha)}, \tag{C3}$$

where $E_{0,p}$ denotes the electric field *inside* the sphere when the dielectric constant of particle is ε_p. Notably when integrating the previous expression over α, the particle dielectric constant ε_p is considered as a *variable* changing from ε_m to ε. The resonant frequency shift $\Delta\omega$ is

$$\Delta\omega = -\frac{\omega V_p}{2\int_{V_c}\varepsilon_c|\vec{E_0}|^2dV}\int_0^{\mathrm{Re}(\alpha)}|\overrightarrow{E_{0,p}}|^2\frac{d\varepsilon_p}{d\mathrm{Re}(\alpha)}d\mathrm{Re}(\alpha). \tag{C4}$$

In the Rayleigh limit, electric field inside the particle is uniform and is proportional to the unperturbed field in the cavity:

$$\overrightarrow{E_{0,p}} = \frac{3\varepsilon_m}{\varepsilon_p+2\varepsilon_m}\vec{E_0}. \tag{C5}$$

Substituting Eq. (C5) into Eq. (C4) we have

$$\begin{aligned}\Delta\omega &= -\frac{\omega V_p|\vec{E_0}|^2}{2\int_{V_c}\varepsilon_c|\vec{E_0}|^2dV}3\varepsilon_m\frac{\varepsilon-\varepsilon_m}{\varepsilon+2\varepsilon_m}\\ &= -\frac{\omega|\vec{E_0}|^2}{2\int_{V_c}\varepsilon_c|\vec{E_0}|^2dV}\mathrm{Re}(\alpha).\end{aligned} \tag{C6}$$

Figure 6 compares the resonant wavelength shift calculated using Eq. (C6) in a 1D cavity along with FDTD simulations, as well as results predicted by other different cavity perturbation methods, including the conventional nondegenerate perturbation theory and the perturbation theory involving shifting material boundaries [14].

In the case of a spherical Rayleigh particle inside a cavity, both Eqs. (A9) and (C6) should lead to the same resonant frequency shift, that is,

$$\Delta\omega = -\frac{\omega|\vec{E_0}|^2}{4N\hbar\omega}\mathrm{Re}(\alpha) = -\frac{\omega|\vec{E_0}|^2}{2\int_{V_c}\varepsilon_c|\vec{E_0}|^2dV}\mathrm{Re}(\alpha). \tag{C7}$$

Comparing the two equations we find

$$N\hbar\omega = \frac{1}{2}\int_{V_c}\varepsilon_c|\vec{E_0}|^2dV. \tag{C8}$$

This means that the time-averaged electric field energy and the magnetic field energy are equal in a standing wave resonant cavity. This conclusion can be alternatively illustrated by considering the standing wave nature of resonant mode. In a high-finesse cavity, the time-averaged power flux is close to zero, that is,

$$\overrightarrow{S} = \tfrac{1}{2}\mathrm{Re}(\vec{E_0}\times\vec{H_0}*) \approx 0. \tag{C9}$$

Equation (C9) essentially specifies that the electric field and the magnetic field have $\pi/2$ phase difference. Therefore, electromagnetic energy oscillates between purely electric to purely magnetic natures in the time domain, and hence the equality of time-averaged electric field energy and the magnetic field energy.

Notably since we have no pre-assumptions regarding the nature of the cavity when deriving Eq. (A9) and Eq. (C6), Eq. (C8) is a general conclusion. This conclusion thus allows us to cast Eq. (A9) in a form identical to Eq. (C6):

$$\Delta\omega = -\frac{\omega|\vec{E_0}|^2}{2\int_{V_c}\varepsilon_c|\vec{E_0}|^2dV}\mathrm{Re}(\alpha). \tag{C10}$$

However, Eq. (C9) is not limited to spherical particles, and thus provides a way to evaluate cavity perturbation due to a dipolar particle of an arbitrary shape.

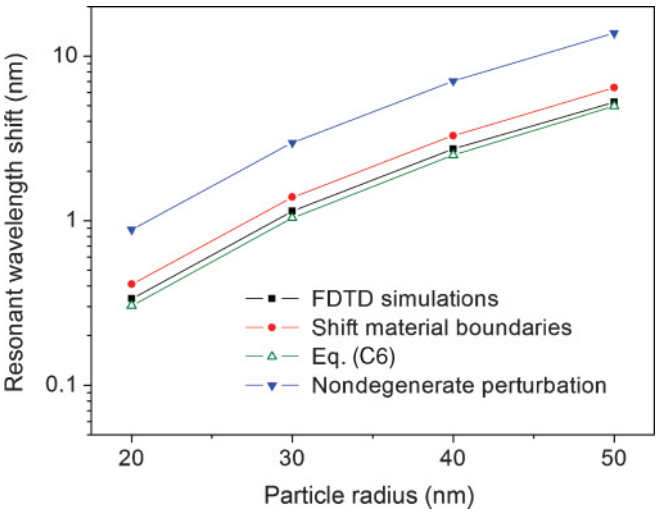

FIG. 6. (Color online) Resonant wavelength shift of a 1D cavity shown in Fig. 1 ($N = 3$) induced by introduction of a particle into the cavity center, calculated 3D FDTD and using different cavity perturbation formalisms; clearly, Eq. (C6) gives theoretical predictions in good agreement with FDTD simulation results.

[1] A. Ashkin, J. M. Dziedzic, J. E. Bjorkholm, and S. Chu, Opt. Lett. **11**, 288 (1986).
[2] M. P. MacDonald, G. C. Spalding, and K. Dholakia, Nature (London) **426**, 421 (2003).
[3] A. H. J. Yang, S. D. Moore, B. S. Schmidt, M. Klug, M. Lipson, and D. Erickson, Nature (London) **457**, 71 (2008).
[4] E. Schonbrun, C. Rinzler, and K. B. Crozier, Appl. Phys. Lett. **92**, 071112 (2008).
[5] E. Schonbrun and K. B. Crozier, Opt. Lett. **33**, 2017 (2008).
[6] A. Rahmani and P. C. Chaumet, Opt. Express **14**, 6353 (2006).
[7] M. Barth and O. Benson, Appl. Phys. Lett. **89**, 253114 (2006).
[8] S. Lin, J. Hu, L. C. Kimerling, and K. B. Crozier, Opt. Lett. **34**, 3451 (2009).
[9] S. Arnold, D. Keng, S. I. Shopova, S. Holler, W. Zurawsky, and F. Vollmer, Opt. Express **17**, 6230 (2009).
[10] M. Eichenfield, C. Michael, R. Perahia, and O. Painter, Nat. Photonics **1**, 416 (2007).

[11] S. Mandal, X. Serey, and D. Erickson, Nano Lett. **10**, 99 (2010).
[12] S. Lin, E. Schonbrun, and K. Crozier, Nano Lett. **10**, 2408 (2010).
[13] K. J. Vahala, Nature (London) **424**, 839 (2003).
[14] M. Nieto-Vesperinas, P. C. Chaumet, and A. Rahmani, Philos. Trans. R. Soc. London A **362**, 719 (2004).
[15] P. Rakich, M. Popovic, M. Soljacic, and E. Ippen, Nat. Photonics **1**, 658 (2007).
[16] S. G. Johnson, M. Ibanescu, M. Skorobogatiy, O. Weisberg, J. D. Joannopoulos, and Y. Fink, Phys. Rev. E **65**, 066611 (2002).
[17] J. Joannopoulos, S. Johnson, J. Winn, and R. Meade, *Photonic Crystals: Molding the Flow of Light*, 2nd ed. (Princeton University Press, Princeton, 2008).
[18] W. T. Doyle, Phys. Rev. B **39**, 9852 (1989).
[19] B. Draine, Astrophys. J. **333**, 848 (1988).
[20] S. Gaugiran, S. Gétin, J. Fedeli, G. Colas, A. Fuchs, F. Chatelain, and J. Dérouard, Opt. Express **13**, 6956 (2005).
[21] D. Englund, D. Fattal, E. Waks, G. Solomon, B. Zhang, T. Nakaoka, Y. Arakawa, Y. Yamamoto, and J. Vuckovic, Phys. Rev. Lett. **95**, 013904 (2005).
[22] Z. G. Xie, S. Götzinger, W. Fang, H. Cao, and G. S. Solomon, Phys. Rev. Lett. **98**, 117401 (2007).
[23] A. Armani, R. Kulkarni, S. Fraser, R. Flagan, and K. Vahala, Science **317**, 783 (2007).
[24] K. L. Kelly, E. Coronado, L. Zhao, and G. C. Schatz, J. Phys. Chem. B **107**, 668 (2003).